

Nonhomogeneous resolution of images of natural scenes

Boubakar Séré, Christian Marendaz[¶], Jeanny Hérault[#]

LPE (CNRS), Laboratory of Experimental Psychology, University Pierre Mendès-France, BP 47, 38040 Grenoble cedex 9, France; e-mail: christian.marendaz@upmf-grenoble.fr;

[#] LIS (CNRS), Institut National Polytechnique de Grenoble, Grenoble, France

Received 11 October 1999, in revised form 10 July 2000

Abstract. The aim of this research is to model and simulate the loss of visual resolution as a function of retinal eccentricity in the perception of natural scenes. The model of visual resolution is based on a space-variant low-pass filter, having a variable convolution kernel according to retinal eccentricity. The parameters of the model are computed from psychophysical measures of visual acuity as a function of retinal eccentricity. The implementation of the model allowed us to generate images of scenes with nonhomogeneous space-variant resolution, simulating the filtering executed by the eye. These scenes are used to test and optimise the model by means of experiments in static vision (through tachistoscopic presentations) and in dynamic vision where the resolution of the scene is computed, in real-time, as a function of the location of gaze.

1 Introduction

The ability to perceive fine details in the visual environment depends on visual acuity—the spatial resolution power of the visual system. Visual acuity is not uniform across the visual field (De Valois and De Valois 1988; Wilson et al 1990). During an ocular fixation, only a very restricted area of the visual field is perceived distinctly (Rayner and Pollatsek 1992). This can be shown if one maintains fixation on a single word in a text: Words adjacent to the fixed word are still readable, but those further away are not. More objective measures from psychophysical and neurophysiological studies show that visual acuity decreases as the inverse of retinal eccentricity (figure 1). In everyday life, however, humans are not aware of this decrease in acuity because of compensating eye movements. But how much do the eyes perceive of natural scenes if one discards eye movements? Previous psychophysical studies do not resolve this question since they used extremely simplified visual stimuli (eg gratings of different spatial frequencies), and since the ensemble of spatial frequencies present in natural scenes have contrast well below those used for measures of visual acuity (eg Hughes et al 1996).

The aim of the present study is to model and simulate the spatial resolution of the eye as a function of retinal eccentricity in the perception of natural scenes. The analysis of biological factors determining visual acuity leads us to ground our model on the principle of low-pass space-variant filters (eg Beaudot et al 1993; Mallot et al 1990). The specification of the parameters of the model as a function of psychophysical measures allows us to create images of natural scenes with nonhomogeneous spatial resolutions, thereby simulating foveal and extrafoveal spatial resolutions of the eye. These images were used to test and optimise the model by experiments in static vision (using tachistoscopic presentations) and in dynamic vision (where the image resolution is defined in real-time as a function of the location of fixation). In these experiments, human observers had to discriminate between original images of natural scenes and images of the same scenes filtered by the model.

[¶] Author to whom correspondence and requests for reprints should be addressed.

2 Modelling and simulating the nonhomogeneous resolution (NHR) of the eye

2.1 Biological determinants of visual acuity

The decrease in visual acuity as a function of retinal eccentricity is essentially due to the nonhomogeneous distribution of retinal photoreceptors and the retinotopic organisation of the primary (striate) visual cortex (Osterberg 1935; Wilson et al 1990). The human retina comprises about 100 million rods and 5 million cones. The distribution of these two types of photoreceptors is nonhomogeneous. Specifically, the density of cones, responsible for vision in photopic conditions, is large in the foveal region and decreases rapidly with retinal eccentricity; also, the receptive fields of the photoreceptors are larger in the perifoveal region. While the organisation of receptive fields of neurons in the primary visual cortex is similar to that of retinal cells, one observes in the primary visual cortex a cortical magnification of neurons coding different local characteristics (Cowey and Rolls 1974; Sereno et al 1995). For example, the processing of the central region of the visual field, spanning 10 deg (or 1/60th of the total surface) takes place in about half the surface of the primary visual cortex. In other words, if one takes as an index of magnification the linear extent of the cortical surface allotted to the processing of 1 deg of visual angle, this index has a value of 30 in the foveal region, compared to 3 at 20 deg of retinal eccentricity (Dow et al 1981; see also Anstis 1998). The functional consequences of these neuroanatomical characteristics mean that the eye appears as a filter whose spatial characteristics vary as a function of retinal eccentricity.

2.2 Model

In order to formalise and simulate the nature of spatial filtering executed by the eyes, we used the psychophysical measures of contrast sensitivity as a function of spatial frequency and retinal eccentricity obtained by Virsu and Näsänen (1978) in static vision (figure 1).⁽¹⁾

Mathematically, contrast sensitivity is the inverse of contrast. The sensitivity curves indicate the level of minimal contrast necessary to perceive a sinusoidal grating of a given spatial frequency and retinal eccentricity (below this threshold, the grating appears as a uniform grey). In the context of these sensitivity measures, visual acuity is

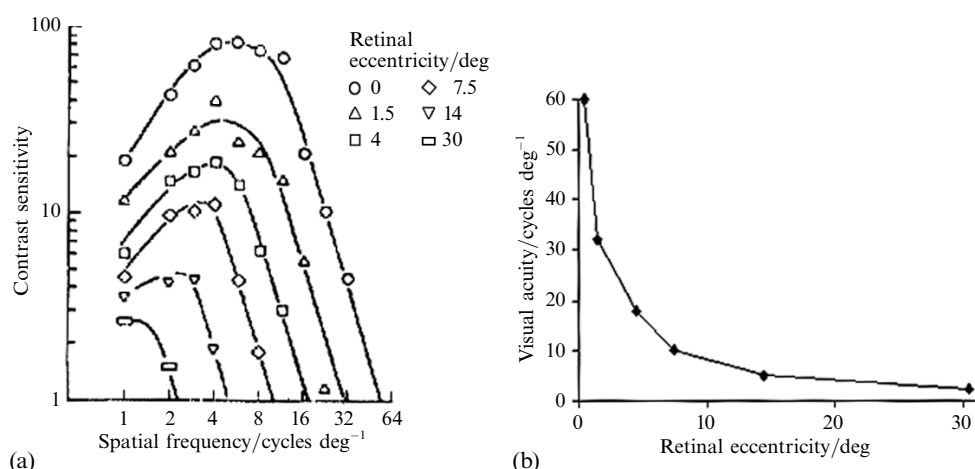


Figure 1. (a) Contrast sensitivity in the human subject as a function of retinal eccentricity (from Virsu and Näsänen 1978). (b) Visual acuity as a function of retinal eccentricity.

⁽¹⁾ Galvin et al (1997) showed that subjects systematically judged a peripheral stimulus as less blurred than it actually is, and termed this effect "peripheral sharpness overconstancy". Since the NHR model is based on experimental data resulting from the psychophysical measurement of visual acuity as a function of retinal eccentricity in human observers, this model takes into account the peripheral sharpness overconstancy effect.

usually defined as the highest spatial frequency at maximum contrast, corresponding in figure 1a to the frequency determined by the intersection of each of the curves with the abscissa. As figure 1b shows, visual acuity rapidly decreases as a function of retinal eccentricity, and it can be shown that the following equation is the best approximation of the relation between visual acuity and retinal eccentricity:

$$A(e) = \frac{A_0}{1 + \beta e}. \quad (1)$$

In this equation, A_0 represents the level of visual acuity in foveal vision, e represents retinal eccentricity (in degrees of visual angle), and β is a parameter which, for the acuity data in figure 1, has a value of 1/1.6. The psychophysical function of acuity as defined shows that the visual system functions as a filter selecting frequency ranges that decrease with retinal eccentricity (which fits with the decreasing receptive field sizes and spatial density of perifoveal receptors described earlier). One can model this property of the visual system using a space-variant low-pass filter whose filtering frequency is a function of retinal eccentricity. This filter is described in the following equation.

$$G(f_x, f_y) = 1 / \left[1 + 4\pi^2 a^2 \left(\frac{f_x^2 + f_y^2}{f_0^2} \right) \right], \quad (2)$$

where f_x and f_y are horizontal and vertical spatial frequencies, respectively, f_0 is the sampling frequency (for example, it represents the inverse of the step between ganglion cells of the retina), and a is a normalised space constant. In accordance with equation (1), this step varies as $(1 + \beta e)/A_0$, giving a transfer function depending on eccentricity:

$$G(f_x, f_y) = \frac{1}{1 + 4\pi^2 a^2 (1 + \beta e)/A_0 (f_x^2 + f_y^2)}, \quad (3)$$

which gives a space constant $a' = [(1 + \beta e)/A_0]^{1/2}$, depending on eccentricity.

2.3 Simulation

Figure 2b represents the space-variant filtering executed by the eye viewing an image scene in figure 2a, with a value of $\beta = 1/1.6$ [cf equation (1)]. Inspection of figures 2a and 2b shows that the decrease in image resolution as a function of retinal eccentricity is very small (the similarity between the original image and the filtered one is enhanced by the reduction in size of the images (their real size is 30 cm × 24 cm). The validity of the model is investigated in experiment 1.

3 Test and optimisation of the NHR model in static vision

3.1 General method

The experimental task used to test the NHR model was the following. Human observers perceived a sequence of two images representing the same natural scene, of which one was filtered according to the NHR model, and the other (the original) was not. Upon viewing each sequence, the participants had to indicate which of the two images was the original (the non-filtered one). Unknown to the observers, half of the sequences in each experiment consisted of two original, non-filtered images. These 'bogus' trials were used in order to control the possibility that the participants were basing their response merely on slight differences in contrast between filtered and non-filtered images. This slight decrease in contrast for the filtered images is an inherent consequence of the low-pass filtering procedure.

A pilot study showed that observers in fact perceived these differences as variations in luminance, where the filtered image appeared less luminous than the non-filtered one. This phenomenon can be explained by the fact that a region of a low-pass filtered image has a lower energy value than its environment (even if the local falls in energy



Figure 2. Simulation of the nonhomogeneous resolution of images as a function of retinal eccentricity. (a) An original, non-filtered image. (b)–(f) Different levels of space-variant filtering tested in experiments 1 and 2. Image (b) corresponds to a filtering based on visual acuity ($\beta = 1/1.6$) and image (d) to the optimised filtering model ($\beta = 3/1.6$). In order to see the effect of space-variant filtering in these small pictures better, the focus of filtering is on the fruit basket (as if the observers fixed their eyes on the fruit basket) while it was on the centre of the image in the experiments. Images should be inspected at a viewing distance of 14 cm.

have been partially compensated by adjusting at each location the gain of the spatially variant filter so that the local mean intensity of the image was preserved), which can be confounded in the periphery by a local decrease in luminance. By inserting bogus trials in the experiments, luminance differences were no longer a reliable criterion for responding. The choice of bogus trials only made up of non-filtered images was also used to improve the subjects' familiarity with these images, and, as a consequence, to increase their perceptual dexterity with them (as opposed to filtered images), in order to compensate for the ambiguity potentially generated by the bogus trials.

3.2 *Experiment 1: Test of NHR model in static vision*

In this experiment we tested the validity of the theoretical NHR filtering method, corresponding to a value of (β of $1/1.6$, as a description of the distribution of spatial resolution as a function of retinal eccentricity. We reasoned that, if this model would be a valid description, then observers should be unable to discriminate between filtered and non-filtered images of natural scenes.

3.2.1 Subjects. Twelve undergraduate students in psychology from the University Pierre Mendès-France in Grenoble participated in this experiment for course credit. All had normal or corrected-to-normal vision and they were not aware of the purpose of the experiment.

3.2.2 Stimuli and procedure. Each trial consisted of a sequence of two images (sized 30 deg \times 24 deg), presented on a 17-inch screen with a resolution of 1024 \times 768 pixels. The images in a sequence represented the same scene, chosen from a collection of eight natural scenes depicted in grey-level (figure 3). Half of the sequences consisted of an original (non-filtered) scene and the same image filtered according to the NHR model; the order of appearance of the images in the sequence was counterbalanced. (These sequences will be termed mixed.) The remaining half of the sequences consisted of two non-filtered images (bogus trials). The participant's task was to determine the original image in each sequence by indicating which of the two images had the 'best resolution'. At the start of experiment, four example trials were administered to illustrate to the participants the difference between filtered and non-filtered images, according to the NHR model.



Figure 3. Set of images used in experiments 1, 2, and 3.

The NHR-filtered images were defined according to their centre (corresponding to the centre of the screen); it was therefore important that the observers fixed their eyes on the centre of the screen throughout a sequence. In order to ensure that the participants were fixating the centre, a secondary task was used in the experiment: Following a 500 ms fixation point, a letter (measuring 0.3 deg) was presented at the centre for 500 ms, and the participants had to verbally identify the letter. Following the displaying of the letter, the first image was presented for 150 ms (in order to avoid ocular saccades). After 1 s, the same procedure was repeated with the second image. Responses were made after viewing the second image. Responses on trials in which the target letter was named incorrectly were discarded from analysis (less than 1%).

The experiment consisted of 480 trials, presented in a randomised order and in four blocks separated by 5 min breaks. The accuracy of the responses to the mixed image sequences—consisting of a filtered and a non-filtered image—was measured. The bogus trials were not included in the analysis.

3.2.3 Results. Let us highlight the fact that none of the observers reported the presence of bogus trials. On average, observers correctly indicated the non-filtered images in 49.89%, which is at chance level. Thus, in this experiment the observers were unable to

discriminate between NHR-filtered and non-filtered images. While this result is consistent with our predictions, it does not necessarily indicate that the filtering by the eyes at different eccentricities is accomplished according to the NHR model. This is because the theoretical model is based on a definition of visual acuity at maximum contrast. Since contrast in natural scenes decreases as a function of the inverse of spatial frequency (eg Hughes et al 1996), the model underestimates the filtering of the eyes. How can the cut-off frequency be determined in a more realistic way? This question is examined in the following experiment.

3.3 Experiment 2: Calculation of the optimal filtering threshold (static vision)

The goal of experiment 2 was to see whether the theoretical model ($\beta_1 = 1/1.6$) underestimates the filtering of the eyes, and, if so, to refine the model by empirically determining the optimal level of filtering. The optimal level of filtering is the value of filtering beyond which the observers are able to reliably discriminate between NHR-filtered and non-filtered images.

3.3.1 *Subjects, stimuli, and procedure.* Twelve undergraduate students in psychology from the University Pierre Mendès-France in Grenoble (different from those of experiment 1) participated in the experiment. The same stimuli and procedure were used as in experiment 1. Additionally, four levels of filtering were used, at different levels of the β parameter: $\beta_2 = 2/1.6$, $\beta_3 = 3/1.6$, $\beta_4 = 4/1.6$, and $\beta_5 = 5/1.6$. These different levels of filtering are illustrated in figures 2c to 2f. These values were chosen following pilot work in which observers ranked different images (presented on sheets) according to their level of filtering. A β value below $1/1.6$ yielded errors in this ranking.

There were 1920 image sequences (480 for each filtering level), of which 50% were mixed trials, and 50% bogus trials. The accuracy of the responses to the mixed image sequences—consisting of a filtered and a non-filtered image—was measured.

3.3.2 *Results.* As in experiment 1, none of the observers reported the presence of bogus trials. Table 1 shows the mean percentage of correct responses (and standard deviations) at mixed trials for each level of filtering ($\beta_2 - \beta_5$). The accuracy of responses for β_2 and β_3 is similar to those obtained in experiment 1. Statistical analysis indicates that the rate of correct responses differs from chance only from the third filtering level [$\chi^2_1 = 29.5$, $p < 0.001$].

One can thus consider the second level of filtering ($\beta_3 = 3/1.6$) as the one corresponding to the filtering accomplished by the eye at different regions in the visual field (figure 2d). Of course, we could try to make the optimal filtering threshold more precise by refining the variation step of β between β_2 and β_4 but, on the one hand, the increased precision would be too low and results of a pilot study showed that observers failed to distinguish increments of β smaller than $1/1.6$, even if they had plenty of time to watch the two images. In the following experiment, we have preferred to try testing the NHR model in a more realistic (ecological) situation, in which observers were allowed to visually explore the displays rather than maintaining fixation throughout a presentation.

Table 1. Percentages of correct responses (with standard deviations) as a function of the level of filtering, β .

	Level of filtering			
	$\beta_2 = 2/1.6$	$\beta_3 = 3/1.6$	$\beta_4 = 4/1.6$	$\beta_5 = 5/1.6$
Correct responses/%	51.5	51.9	88.4	86.9
Standard deviations/%	3.5	3.4	6.3	4.5

3.4 Experiment 3: Testing the NHR model in free vision

In order to test the NHR model under free vision conditions, ie by allowing observers to make eye movements, we used a setup that allowed us to adjust, in real-time, the filtering of the image as a function of the location of fixation. If the NHR model is an adequate description of ocular filtering at different eccentricities, the observers should not be able to discriminate between original non-filtered images, and images filtered according to the NHR model.

3.4.1 Apparatus and stimuli. Eye movements were monitored by an oculometer system ('Eyeputer') at a sampling rate of 480 Hz, and a spatial resolution of about 0.1 deg. A frame was used to immobilise the observer's head during the experiment (figure 4).



Figure 4. Illustration of experiment 3 (free vision). Ocular fixations (monitored by an oculometer 'Eyeputer') determine, in real-time, the focus of the space-variant filtering of the image.

Filtering the images in real-time according to the observers' gaze location poses problems with regard to the timing of the onset and duration (presentation time) of the image. First, concerning the duration, it is practically impossible to filter an image anew at each new fixation without substantial temporal delays. In order to circumvent this problem, we calculated filtering according to fixed (imaginary) positions of fixation in the following way. The screen was divided into 64 (8×8) imaginary sections, each $3.75 \text{ deg} \times 3.0 \text{ deg}$ in size and, for each section, a filtered image was created with the low-space-variant filtering ($\beta = 3/1.6$) located at the centre of the section. The 64 images thus prepared were stored in a buffer which allowed presentation on the screen within a screen refresh (14 ms). Secondly, concerning the timing of the onset of the image, this needs to be accomplished so that the observer is unaware of the change. There are two solutions. The first one is to display the filtered image during a saccadic eye movement, since the change will be imperceptible owing to saccadic suppression (ie the reduced sensitivity of the eyes to visual stimulation during saccades; Burr et al 1994; Volkman 1986). One problem with this solution, however, is that the filtering of the image during a saccade must be in congruence with the location of gaze following the saccade (since the filtering is determined by retinal eccentricity). In other words, one must predict the location of fixation following a saccade, and this is difficult to achieve with a sufficient degree of accuracy. Therefore, we opted for a second solution, in which the image is presented right at the end of a saccadic eye movement, at the next fixation. Following this fixation, there is a time window of about 20–40 ms during which the threshold for the detection of changes in stimuli is elevated (Charbonnier et al 1995). This time window at fixation can be used to produce the onset of the filtered image within a screen refresh of 14 ms, thus falling within the time window, and while knowing accurately the location of fixation.

The onset of a filtered image was achieved as follows. When the onset of a saccadic eye movement was detected, the computer system determined the section of the image in which the following fixation would fall, and the filtered image according to the new fixation was presented. The saccadic onset was determined by continuous measures of the eye-movement registration system. The onset of a saccade was determined by measuring deviations in eye position from a predetermined threshold; below this

threshold the system assumed the eye was fixed. The threshold for detecting saccades was determined in a pretest for each observer by measuring the distribution of the locations of the centre of gravity of the pupil in an ocular pointing task.

3.4.2 Subjects and procedure. Fourteen undergraduate students in psychology from the University Pierre Mendès-France in Grenoble participated in the experiment. The observer's task was to freely explore each scene image for 1 min, and report the subjective distinctness of the image. Observers were not informed about the image-filtering manipulation. Each scene exploration started from a fixed central point on the screen. The size of each image was 30 deg \times 24 deg. The experiment had three image-filtering conditions, which were manipulated within-subjects. From one fixation to the next, the scene presented consisted of either (i) original (non-filtered) images, (ii) filtered images (cf figure 2d), or (iii) a succession of an original and a filtered image (in counterbalanced order); in this last condition, stimulus alternated between a filtered and a non-filtered image on successive saccades.

3.4.3 Results. When the viewed scene was composed solely of filtered or original images [conditions (i) and (ii)], the observers reported the scene as being distinct. In contrast, when original and filtered images were presented in succession across saccades [condition (iii)], 13 out of 14 observers reported a subjective visual change of the image (reporting that "something changed in the image"), but without being able to report what exactly had changed. None of the observers reported that the images were filtered (these were shown to them at the end of the experiment). One could think that the perceived change in image was due to differences in mean contrast between the filtered and original images (cf discussion in section 3.1 above). However, these results neither invalidate the NHR model nor the procedure adopted to present the filtered images. Of course, this type of experiment needs to be pursued in order to make the optimal filtering threshold in dynamic vision more precise. This 'time-consuming' research is planned.

4 General discussion

In spite of the empirical evidence from psychophysics and neuroscience showing a decrease of visual acuity as a function of retinal eccentricity, it is difficult to visualise this peripheral acuity (Anstis 1998) owing to the problem of representing the change which the input signal undergoes in the periphery of the retina. This is especially true with complex images of natural scenes. The aim of this study was to simulate this image representation on the basis of a space-variant filtering model (NHR). This model was based on known psychophysical data of acuity (Virsu and Näsänen 1978) and tested and optimised by empirical data in static and dynamic vision.

It should be underlined that the NHR model is intended as a heuristic model not as a veridical representation of what is perceived across the visual field, since it is nearly impossible to design an experimental proof of this. Moreover, the model does not take into account more fine-grained and complex variations in visual acuity as, for example, slight disparities in cortical magnification between the lower and upper visual field as a function of retinal eccentricity (see Anstis 1998, for further details).

In its present version, the NHR model offers a solution to the problem of the presentation of large-size images in the context of virtual reality. Displaying such images is costly in terms of computer memory. Until now, bi-resolution models have been proposed based on the principle of superimposing the high-resolution central part of an image onto the rest of the image which is in low resolution (Abdel-Malek and Bloomer 1990; Iwamoto et al 1994; Peters 1994). These models suffer from the drawback that they disturb a smooth perception of scenes, and hence they lack realism.

The NHR model, which can easily be applied to colour images, may constitute a more realistic solution.

To conclude, the simulations of the NHR model also allow a better understanding of coarse-to-fine processing in very fast scene recognition (Fabre-Thorpe et al 1998; Hughes et al 1996; Marendaz et al, in press; Parker et al 1992). Coarse-to-fine processing refers to the precedence of low-spatial-frequency processing of scenes over high-spatial-frequency processing. Low-spatial-frequency processing enables the visual system to make categorical inferences based on the coarse spatial structure of a scene (Schyns and Oliva 1994, 1997). At a neurophysiological level, this model is interpreted as a consequence of the temporal dynamics of spatial-frequency channels which transmit information of low spatial frequencies more rapidly than of high spatial frequencies (Hérault et al 1997). Our simulations (see also figure 5 which reproduces what the eye would see of a scene of $120\text{ deg} \times 135\text{ deg}$ corresponding to the size of the stereoscopic vision) show that coarse-to-fine analysis of natural scenes is actually a strategy which is better adapted to the information available in early vision. One could imagine that the temporal dynamics of spatial-frequency channels is, from the viewpoint of evolution, not a cause but rather a consequence of coarse-to-fine image processing, this processing proceeding from the spatially varied filtering operated by the eyes.

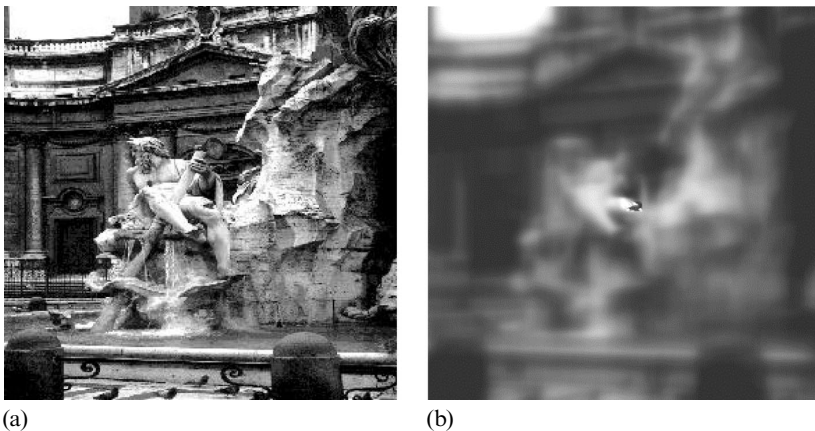


Figure 5. Image (b) reproduces what, according to the NHR model, the eye would perceive of the original, non-filtered scene (a) if this had a size of $120\text{ deg} \times 135\text{ deg}$ (1 cm on the image is about 27 deg visual angle) corresponding to the size of stereoscopic vision. The image should be inspected at a viewing distance of 14 cm.

Acknowledgements. Preparation of this article was supported by Pierre Mendès-France University, the CNRS, and the CNET. We thank S Thorpe and the anonymous reviewers for comments on this manuscript.

References

- Abdel-Malek A, Bloomer J, 1990 "Visually optimized image reconstruction" *SPIE: Human Vision and Electronic Imaging: Models, Methods and Applications* **1249** 330–335
- Anstis S M, 1998 "Picturing peripheral acuity" *Perception* **27** 817–825
- Beaudot W, Palagi P, Hérault J, 1993 "Realistic simulation tool for early visual processing including space, time and colour data", in *New Trends in Neural Computation* Eds J Mira, J Cabestany, A Prieto (Heidelberg: Springer) pp 370–375
- Burr D C, Morrone M C, Ross J, 1994 "Selective suppression of the magnocellular visual pathway during saccadic eye movements" *Nature (London)* **371** 511–513
- Charbonnier C, Marendaz C, Hollard S, Massé D, 1995 "Gaze-controlled display" *Perception* **24** Supplement, 92
- Cowey A, Rolls E T, 1974 "Human cortical magnification and its relation to visual acuity" *Experimental Brain Research* **21** 447–454
- De Valois R L, De Valois K K, 1988 *Spatial Vision* (New York: Oxford University Press)

- Dow B M, Snyder A Z, Vautin R G, Bauer R, 1981 "Magnification factor and receptive field size in fovea striate cortex of the monkey" *Experimental Brain Research* **44** 213–228
- Fabre-Thorpe M, Richard G, Thorpe S, 1998 "On the speed of scene categorisation in human and non-human primates" *Current Psychology of Cognition* **17** 791–807
- Galvin S J, O'Shea R P, Squire A M, Govan D G, 1997 "Sharpness overconstancy in peripheral vision" *Vision Research* **37** 2035–2039
- Hérault J, Oliva A, Guerin-Dugue A, 1997 "Scene categorisation by curvilinear component analysis of low frequency spectra" *Proceedings of the 5th European Symposium on Artificial Neural Networks* (Bruges Belgium) pp 91–96
- Hughes H, Nozawa G, Kitterle F, 1996 "Global precedence spatial frequency channels and the statistics of the natural image" *Journal of Cognitive Neuroscience* **8** 197–230
- Iwamoto K, Katsumata S, Tanie K, 1994 "An eye movement tracking-type head mounted display for virtual reality systems: evaluation experiments of a prototype system" *IEEE International Conference on Systems, Man and Cybernetics* pp 13–18
- Mallot H A, Seelen W V, Fotios G, 1990 "Neural mapping and space-variant image processing" *Neural Networks* **3** 245–263
- Marendaz C, Rousset S, Charnallet A, in press "Reconnaissance des scènes, des objets et des visages", in *Perception et Réalité* Eds A Delorme, M Flückiger (Montréal: Gaëtan Morin)
- Osterberg G A, 1935 "Topography of the layer of rods and cones in the human retina" *Acta Ophthalmologica* **6** Supplement, 1–102
- Parker D, Lishman J, Hughes J, 1992 "Temporal integration of spatially filtered visual images" *Perception* **21** 147–160
- Peters D L, 1994 "Chasing the eye: An eye-tracked display for the simulation industry. The how and the why" *SID91* 495–498
- Rayner K, Pollatsek A, 1992 "Eye movements and scene perception" *Canadian Journal of Psychology* **46** 342–376
- Schyns P, Oliva A, 1994 "From blobs to boundary edges: Evidence for time- and spatial-scale-dependent scene recognition" *Psychological Science* **5** 195–200
- Schyns P, Oliva A, 1997 "Flexible diagnosticity-driven, rather than fixed perceptually determined scale selection in scene and face recognition" *Perception* **26** 1027–1038
- Sereno M I, Dale A M, Reppas J B, Kwong K K, Belliveau J W, Brady T J, Rosen B R, Tootell R B, 1995 "Borders of multiple visual areas in human revealed by functional magnetic resonance imaging" *Science* **268** 889–893
- Virsu V, Näsänen R, 1978 "Cortical magnification factor predicts the photopic contrast sensitivity of peripheral vision" *Nature (London)* **271** 54–56
- Volkman F C, 1986 "Human visual suppression" *Vision Research* **26** 1401–1416
- Wilson H R, Levi D, Maffei L, Romano J, De Valois R, 1990 "The perception of form. Retina to striate cortex", in *Visual Perception: The Neurophysiological Foundations* Eds L Spillmann, J S Werner (San Diego, CA: Academic Press) pp 231–272